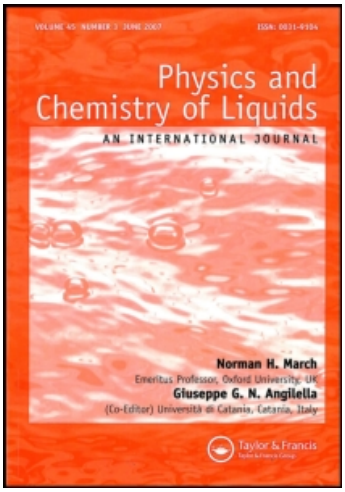

Physics and Chemistry of Liquids
Publication details, including instructions for authors and subscription information:
http://www.informaworld.com/smpp/title~content=t713646857

Structure of molten bi-cu alloys by means of cold neutron scattering in the region of small momentum transfer

Werner Zaiss[ab]; Siegfried Steeb[a]; Günter S. Bauer[c]
[a] Max-Planck-Institut für Metallforschung, Institút für Werkstoffwissenschafter, Stuttgart, Western Germany [b] University of Stuttgart, [c] Institut für Festkörperforschung der KFA, Jülich

Online publication date: 18 October 2010

To cite this Article Zaiss, Werner , Steeb, Siegfried and Bauer, Günter S.(1976) 'Structure of molten bi-cu alloys by means of cold neutron scattering in the region of small momentum transfer', Physics and Chemistry of Liquids, 6: 1, 21 — 41
To link to this Article: DOI: 10.1080/00319107608085058
URL: http://dx.doi.org/10.1080/00319107608085058

Phys. Chem Liq., 1976, Vol. 6, pp. 21–41.

Printed in Dordrecht, Holland

Structure of Molten Bi-Cu Alloys by Means of Cold Neutron Scattering in the Region of Small Momentum Transfer

WERNER ZAISS,†

and

SIEGFRIED STEEB

Max-Planck-Institut für Metallforschung,
Institut für Werkstoffwissenschaften, Stuttgart, Western Germany

and

GÜNTER S. BAUER

Institut für Festkörperforschung der KFA, Jülich

(*Received April 12, 1976*)

In the present work scattering experiments with cold neutrons are described, which were done with molten Bi-Cu alloys in the region of small momentum transfer ($0.08\ \text{Å}^{-1} < \varkappa < 1.5\ \text{Å}^{-1}$). Using the time-of-flight method of analysis for the scattered neutrons, the inelastically scattered neutrons were separated from the elastically scattered neutrons. The coherent scattering cross section was obtained by integration as the area below the quasielastic line and shows a strong increasing tendency with smaller momentum transfer, especially for the molten alloys in the mid-concentration region. This can be explained by the existence of regions with one kind of atoms within the molten alloys.

These inhomogeneities are considered from a more dynamic point of view according to Ornstein and Zernike as concentration fluctuations, the correlation length of which can be determined to be approximately 2Å. Using the more static interpretation according to Guinier, the regions can be regarded as so-called clusters with spherical shape. These clusters consist either of Cu or of Bi atoms and have a diameter of about 6Å, which corresponds to the diameter of the first coordination shell.

With a melt containing 50 at.% Bi, the scattering cross section in the direction of the primary beam decreases by about 40% when the temperature is increased from 800 to 1100°C, the diameter of inhomogeneities remaining nearly constant.

---

† Part of the thesis work of W. Zaiss, University of Stuttgart, 1975.

1 INTRODUCTION

The structure of molten Bi-Cu alloys was investigated in Ref.[1] by diffraction of thermal neutrons ($\lambda_0 = 1.2$ Å) with the result that the melts in the mid-concentration region show a tendency to segregation. Therefore, it was of interest to investigate the region of small momentum transfer ($\kappa < 1.5\,\text{Å}^{-1}$) for the existence of scattering effects caused by this tendency to segregation.

Scattering experiments on molten binary alloys showing a tendency to segregation were described in Refs.[2,3,4]. In Ref.[2] the critical opalescence in the Bi-Ga, Bi-Zn, and Ga-Pb systems was investigated by means of cold neutron scattering. In Refs.[3,4], on the other hand, the method of small angle X-ray scattering was used for the detection of segregated regions within molten Al-Sn and Al-In alloys, respectively. Since Bi has a rather large cross section for X-ray absorption, the optimum thickness of the melts under investigation would be far below 0.1 mm. Therefore, the present investigation with molten Bi-Cu alloys was carried out using cold neutrons ($\lambda_0 = 8$ Å), since with the technique of neutron scattering, the specimen thickness can be up to several millimeters. The experiments were done with the aid of the disorder scattering spectrometer at the KFA Jülich[5].

2 THEORETICAL BACKGROUND

For historical reasons most of the theoretical background for the description of scattering effects in the region of small and very small momentum transfer is to be found in literature under the item "small angle X-ray scattering"[6]. Using cold (long-wavelength) neutrons as a probe led to corresponding momentum transfer also at larger scattering angles.

Strong scattering effects are always observed in these κ-regions, if the specimen contains regions whose scattering length is different from that of the surroundings ("formation of clusters"). Such segregation at the atomic level is also possible within the homogeneous liquid solution of binary molten alloys. Since the differential scattering cross section can be calculated as the square of the scattering amplitude. The part of the differential cross section caused by fluctuations can in general be described according to Schmatz *et al.*[7] as a fluctuation of scattering length density $\eta(\underline{r})$:

$$\frac{d\sigma(\kappa)}{d\Omega} = \frac{1}{N}\left| \int_V [\eta(\underline{r}) - \bar{\eta}]\, e^{i\kappa\underline{r}} dr \right|^2 \tag{1}$$

$$\eta(\underline{r}) = \sum_{i=1}^{N} \delta_i \delta(\underline{r} - \underline{r}_i) \tag{2}$$

with δ_l = scattering length of the nucleus at position $\underline{r}_l$
N = Number of scattering nuclei in the irradiated volume V
$\bar{\eta}$ = mean scattering length density
$\underline{\kappa}$ is the difference between the wave vector $\underline{k}_0$ of the incident and the wave vektor $\underline{k}_1$ of the scattered neutrons:

$$\underline{\kappa} = \underline{k}_0 - \underline{k}_1 \tag{3}$$

Since theoretical treatments of the description of fluctuations in scattering length density in melts are not yet known, the scattering cross section for finite values of κ will be calculated in two ways: firstly, on the assumption of concentration fluctuations, that means with a more dynamic model (Ornstein-Zernike method); and secondly, on the assumption of segregated regions, i.e. with a more static model (Guinier method).

However, it is possible to calculate the scattering cross section for zero momentum transfer, i.e. $\kappa = 0$.

2.1 Calculation for $\kappa = 0$

The scattering cross section for coherent scattering can be obtained from Eq. (4):

$$\left.\frac{d\sigma(\kappa)}{d\Omega}\right|_{COH} = \langle b\rangle^2 S_{NN}(\kappa) + (\Delta b)^2 S_{CC}(\kappa) + 2\Delta b\langle b\rangle S_{NC}(\kappa) \tag{4}$$

with $\langle b\rangle = c_1 b_1 + c_2 b_2$
c_i = atomic concentration of component i ($\sum c_i = 1$)
b_i = mean scattering length of component i
$\Delta b = b_1 - b_2$
It should be noted in connection with Eq. (4) that for scattering with melts the wave vector κ may be replaced by its absolute value. The terms S_{NN}, S_{CC}, and S_{NC} for $\kappa = 0$ have the following meaning according to [9]:

$$S_{CC}(0) = N \cdot \overline{(\Delta c)^2} \tag{5}$$

$$S_{NN}(0) = \frac{\overline{(\Delta N)^2}}{N} + \delta^2 \cdot S_{CC}(0) \tag{6}$$

$$S_{NC}(0) = -\delta \cdot S_{CC}(0) \tag{7}$$

with

$$\delta = \frac{N}{V} \cdot \left(\frac{\partial V}{\partial c}\right)_{P,N,T} \tag{8}$$

$\overline{(\Delta c)^2}$ is the mean square deviation of the concentration and $\overline{(\Delta N)^2}$ the mean square fluctuation of number density within the volume V. With the aid of Eqs. (5) to (8) the coherent scattering cross section for $\kappa = 0$ can

be calculated as follows:

$$\left.\frac{d\sigma(0)}{d\Omega}\right|_{COH} = \langle b\rangle^2 \frac{\overline{(\Delta N)^2}}{N} + N\,\overline{(\Delta c)^2}\,[b\cdot\delta - (\Delta b)]^2 \tag{9}$$

According to this equation, $\frac{d\sigma(0)}{d\Omega}$ is determined by the concentration and density fluctuations existent within the melt. Using the thermodynamic relationships formulated in Ref.[10] Eq. (9) gives Eq. (10):

$$\left.\frac{d\sigma(0)}{d\Omega}\right|_{COH} = \langle b\rangle^2 \rho_0 k_B T \chi_T + F\cdot\left[\frac{c_i}{a_i}\cdot\left(\frac{\partial a_i}{\partial c_i}\right)_{T,P}\right]^{-1} \tag{10}$$

with

$$F = \left(\frac{\rho_0}{\rho_1\rho_2}\right)^2 c_1 c_2 (\eta_1 - \eta_2)^2 \tag{11}$$

and ρ_0 = mean number density of the alloy
ρ_1, ρ_2 = partial number density of component 1 or 2 in the alloy
$\eta_i = \rho_{0,i}\cdot b_i$ = scattering length density for component i
$\rho_{0,i}$ = mean number density of component i
k_B = Boltzmann's constant
χ_T = isothermal compressibility
a_i = thermodynamic activity of component i

For the purpose of discussing Eq. (10), the first term on the right side is now expressed as follows (comp. Ref.[11]):

$$\frac{\overline{(\Delta N)^2}}{N} = \rho_0 k_B T\left(\chi_S + \chi_T\cdot\frac{c_P - c_v}{c_P}\right) \tag{12}$$

with χ_S = adiabatic compressibility
c_P = specific heat at constant pressure
c_V = specific beat at constant volume

According to Eq. (12) the density fluctuations can be expressed in the form of two independent contributions. The first part of Eq. (12) describes the propagating contributions, which are caused by longitudinal adiabatic sound waves. These propagating contributions give rise to inelastic scattering (Brillouin doublet).

The second part of Eq. (12) on the other hand contains the nonpropagating *thermal fluctuations*. These local temperature fluctuations cause quasielastic scattering. The half width of the quasielastic peak thus formed is proportional to the thermal diffusion coefficient.

The second term of the right side of Eq. (10) describes the local, i.e. nonpropagating *concentration fluctuations* which cause quasielastic scattering.

The scattering cross section for this contribution depends on the partial atomic densities of the components ("atomic volume effect"), but is also proportional to the squared difference of the scattering lengths.

2.2 Method of evaluation for $\kappa \neq 0$

a. Ornstein-Zernike method In the neighbourhood of the liquid-gas phase transition within one component liquids long-range density fluctuations occur, the local temperature fluctuations, however, dominating over the propagating density fluctuations. This is the case, since in this region c_P as well as χ_T reach rather large values, whereas c_v remains finite (comp. Eq. (12)). The scattering effect resulting for these conditions is known in optics as critical opalescence. Analogously, local concentration fluctuations with submicroscopical dimensions occur in binary liquids above the liquidus[12]. Ornstein and Zernike[13] were the first to calculate a correlation function for a liquid near the liquid-gas phases. The Fourier transform of this function was used by Fisher[14] to determine the cross section of the concentration fluctuations:

$$\left.\frac{d\sigma(\kappa)}{d\Omega}\right|_{COH}^{c} = \frac{F \cdot \left[\frac{c_1}{a_1} \cdot \left(\frac{\partial a_1}{\partial c_1}\right)_{T,P}\right]^{-1}}{1 + \xi^2 \kappa^2} \tag{13}$$

ξ is the so-called correlation length. Eq. (13) in this form is only valid for small κ.

b. Guinier method The theory developed by Guinier[6] for the scattering of colloidal solutions was applied for the first time in Ref.[3] to binary melts with a tendency to segregation. The main difference between colloidal solutions and such metal melts lies in the fact that the lifetime of inhomogeneities (clusters) within melts is very small compared to that within colloids. Nevertheless, on a time average it is possible to deduce the magnitude and concentration of these clusters from scattering experiments.

The melt has to be considered a two-phase system in which particles with scattering length density η_p and concentration w_p on the one hand and the matrix with scattering length density η_m and concentration $(1 - w_p)$ on the other exist in a homogeneous distribution. The corresponding scattering cross section follows as[6,15]:

$$\left.\frac{d\sigma(\kappa)}{d\Omega}\right|_{COH}^{p} = \frac{1}{\rho_0} w_p (1 - w_p) \cdot V_p (\Delta\eta)^2 \overline{i^2}(\kappa) \tag{14}$$

with $\Delta\eta = \eta_p - \eta_m$

V_p = volume of one particle

$i(\kappa)$ = form factor of one particle ($\overline{i^2(0)} = 1$)

For the validity of Eq. (14) it is necessary that the particles have no size distribution.

Furthermore, it is valid only for dilute systems without interparticular interference[16]. For small κ Guinier's approximation gives

$$\overline{i^2(\kappa)} = \exp\left[-\frac{1}{3}R_g^2 k^2\right] \tag{15}$$

R_g is the radius of gyration. For the case that the scattering particles are spheres with constant density within each sphere, the radius of the sphere R_p may be calculated as

$$R_p = \sqrt{\frac{5}{3}} R_g \tag{16}$$

2.3. Fundamental consideration of the scattering of cold neutrons by melts

Scattering processes within melts are inelastic or quasielastic (see Ref.[11]), i.e., neither coherent nor incoherent elastic scattering is observed. From Eq. (3) the momentum transfer for the scattering process can be obtained as

$$\hbar\underline{\kappa} = \hbar\underline{k}_0 - \hbar\underline{k}_1 \tag{17}$$

The energy transfer is obtained as

$$\hbar\omega = E_0 - E_1 = \frac{\hbar^2}{2m}(k_0^2 - k_1^2) \tag{18}$$

with m = neutron mass.

Figure 1 shows the combinations of $\hbar\omega$ and $\hbar\kappa$ allowed by Eqs. (16) and (17) for the wavelength $\lambda_0 = 8$Å ($E_0 = 1.3$ meV), the parameter being the scattering angle 2θ.

A detector located at the scattering angle 2θ can detect scattered neutrons if the curve for this angle in Fig. 1 passes through regions in which the scattering function of the specimen deviates from zero. For liquids this always is valid for all κ in the region $\hbar\omega \to 0$, where quasielastic scattering takes place, or for inelastic scattering with high frequency modes. As an example, Fig. 1 shows the results for molten Al[17] (instead of molten Cu) and for molten Bi[18]. Both curves are connected by a hatched region, drawn schematically, by which attention may be drawn to the fact that for melts no distinct dispersion relations hold.

Intersections in the region $\hbar\omega > 0$ mean energy-loss scattering of the neutrons, intersections in the region $\hbar\omega < 0$ mean energy-gain scattering. The maximum energy loss of a neutron during one scattering process cannot

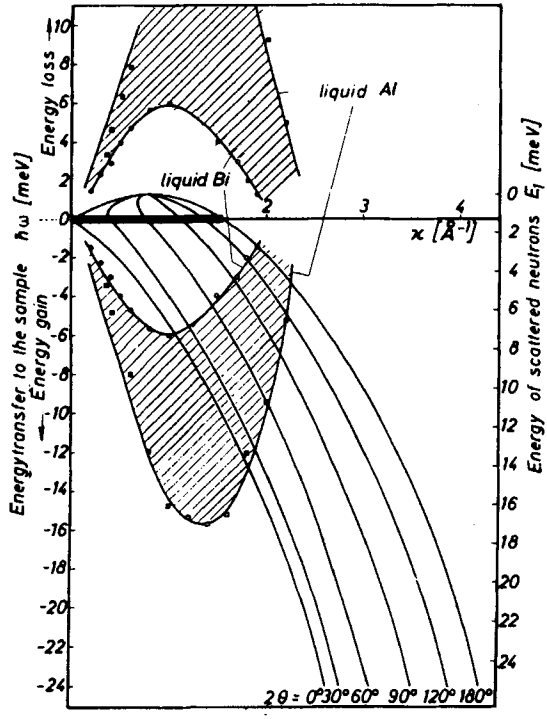

FIGURE 1 Combinations of momentum transfer $\hbar\kappa$ and energy transfer $\hbar\omega$ for a primary neutron energy $E_0 = 1.3$ meV.

be greater than its primary energy. For this case, according to Eqs. (18) and (17) the neutron will loose its total momentum and all curves for all scattering angles will intersect at the point $\hbar\omega = E_0$ and $\kappa = k_0$. Energy-loss scattering (see Figure 1) can be supressed by a convenient choice of incident energy E_0 of the neutrons. However, scattering by energy gain of the neutrons always can take place, since intersections of the energy-transfer curve with the hatched regions in Figure 1 may always exist throughout the region $\hbar\omega < 0$. It is therefore necessary, for example, with the neutrons ($\lambda_0 = 8$Å) used in the present work, to separate the inelastic and the quasielastic scattered neutrons. This is done by pulsing the primary beam and carrying out time-of-flight analysis on the scattered neutrons. One κ-value, namely $4\pi\frac{\sin\theta}{\lambda_0}$ can be ascribed to the integral over the quasielastic peak, which is a measure of the scattering cross section of the local fluctuations.

3 EXPERIMENTAL OUTLINE

The experiments with long-wavelength neutrons ($\lambda_0 = 8$Å) were done on the disorder scattering spectrometer of the KFA Jülich. The spectrometer, originally developed for elastic diffuse neutron scattering, can be used for the determination of differential scattering cross sections of liquids, since it yields rather high scattered intensities, which are preferred to high angular resolution. Thus, the measurements can be done during acceptable lengths of time. The spectrometer itself is described in Ref.[5] and is shown in a schematic diagram in Figure 2. Using the mechanical velocity selector, the desired wavelength can be obtained from the original spectrum. For a desired wavelength of $\lambda_0 = 8$Å, the selector must rotate with 2200 rpm. A Fermichopper which pulses the beam at a frequency of 305 cps is mounted in front of the specimen. The detection of scattered neutrons is done by 30 BF_3 counters mounted at certain positions at a distance L = 80 cm between scattering angles of 2θ between 6° and 147.2°. For time-of-flight analysis, the detectors are used together with 64 time channels with a channel width of 46 μsec for each channel.

The furnace allows experimental temperatures up to 1300°C with a homogeneous temperature distribution at the specimen site. To avoid elastic

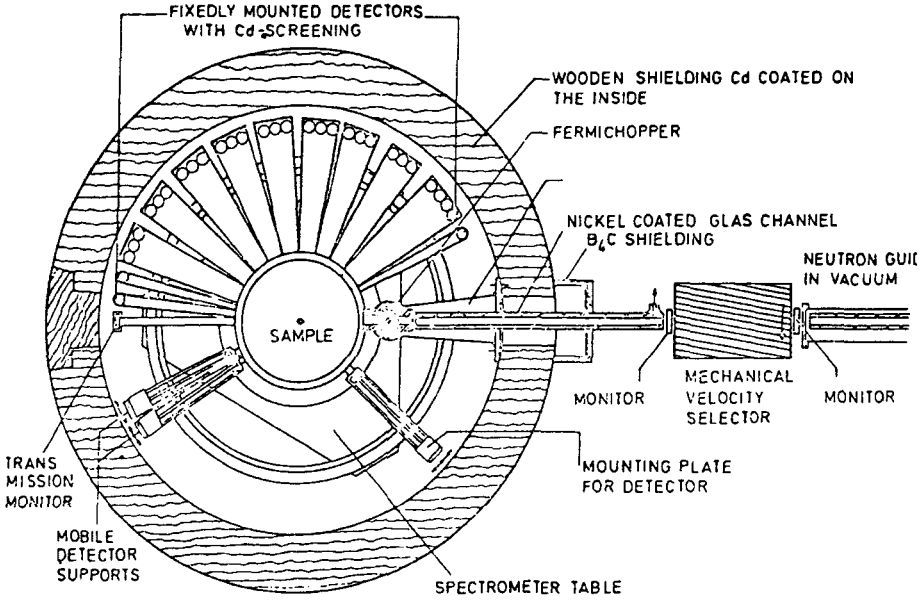

FIGURE 2 Horizontal section through the disorder scattering spectrometer at the height of the experimental plane[5].

background scattering, niobium, which has a small incoherent scattering cross section, is used as the material for the directly heated furnace tube. The other parts of the furnace which could be reached by neutrons are also made of niobium[19]. Replacement of the furnace tube, which is necessary after each 80 hours, is possible without any special readjustment. Also, the specimens can be changed while the furnace is at high temperature. The temperature is controlled electronically, a NiCr-Ni thermocouple just below the specimen inside the furnace tube being used as a sensor. The specimen temperature was measured by a second thermocouple mounted directly at the specimen site.

Since mainly the scattering cross section in the direction of the primary beam is to be determined from the measurements, flat specimens with a thickness of 4 mm are used. The alloys were melted under vacuum in an induction furnace and cast into a cooled rectangular graphite mold 4 mm thick, 32 mm wide, and 90 mm high. Afterwards, the specimen was refined by an ultrasonics treatment. The containers were made of molybdenum, since this material has a rather small incoherent scattering cross section and therefore shows only a small scattering background at the position of the elastic line. The plane-parallel rectangular containers were produced by electron beam welding[20].

The experiments were done automatically. All measurements were made using a constant pulse number set on a monitor counter which was mounted between the velocity selector and the chopper. This was possible since the reference scatterer as well as the melt showed equal scattering rates.

After the furnace had reached the experimental temperature the specimen was lowered into the furnace into a vertical position. Since with this arrangement the counting rate for the detectors at $2\theta \approx 90°$ was seriously influenced by absorption within the specimen and the specimen holder, the specimen had to be turned around 45° so that these counters were also illuminated. The beam itself was collimated using gadolinium and cadmium foils such that neither the frame of the container nor the specimen holder was irradiated, regardless of the position of the specimen. The beam was rectangular with the dimensions 15×70 mm. One run lasted approximately 2 hours; in each position the specimen was measured four times, thus altogether one specimen was under investigation for about 16 hours. To slow down the oxidation of the niobium heating tubes, the furnace was kept under vacuum conditions (10^{-5} torr). For evaluation purposes, an empty molybdenum container also had to be investigated.

Furthermore the measured data had to be normalized to the scattering of vanadium. Using a plate made of vanadium with the same dimensions as the specimens, the beam would experience large absorption and multiple scattering. Thus, a sandwich was used made from six sheets of vanadium, each

0.1 mm thick. The width and height was the same as with the specimens, thus a correction for geometric effects could be avoided.

The attenuation coefficient Σ necessary for calculating the absorption correction was determined in a transmission experiment and is plotted versus the alloy concentration in Figure 3. The absorption correction was made using the formalism given in Ref.[21]. The correction for background was made using the scattering data of the empty molybdenum container.

The probability for the occurence of multiple quasielastic scattering is rather high, if the inequation $0 < \kappa_M < 2\ k_0$ is fulfilled, κ_M being the position of the main maximum in the intensity curve of the melt. According to Ref.[1], for molten Bi-Cu alloys κ_M lies between 2.2 $Å^{-1}$ and 3.0 $Å^{-1}$. Since $\lambda_0 = 8$ Å, for $2k_0$ we get 1.58 $Å^{-1}$, which is smaller than κ_M. Thus, in the present case practically no multiply scattered neutrons may occur near κ_M and therefore no correction for multiple scattering is necessary.

The differential cross section for coherent scattering per atom of the

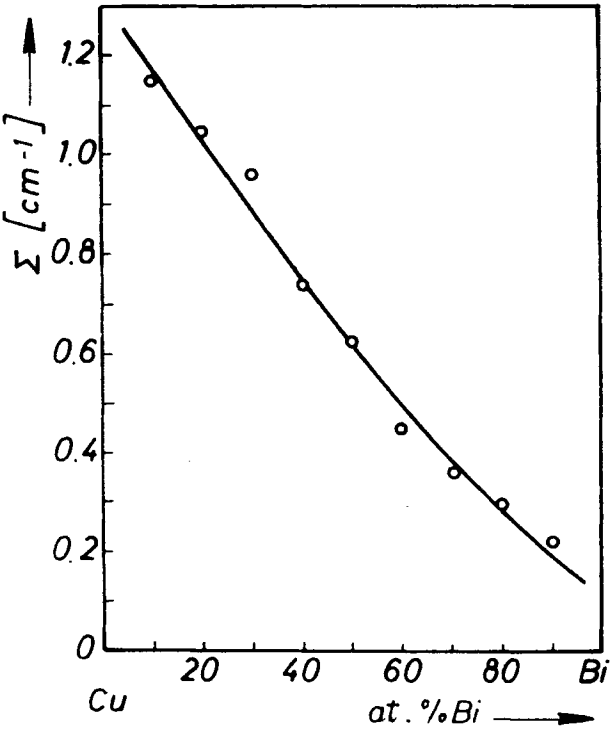

FIGURE 3 Coefficient of attenuation Σ for temperatures of 5° C above liquidus.

melt under investigation is obtained from Eq. (19):

$$\left.\frac{d\sigma(\kappa)}{d\Omega}\right|_{COH} = \frac{1}{4\pi}\left\{\frac{\rho_V}{\rho_0}\frac{I_{COR}^{Sp}}{I_{COR}^{V}}\sigma_{INC}^{V} - c_{Cu}\sigma_{INC}^{Cu}\right\} \tag{19}$$

with ρ_V = number density of vanadium

I_{COR}^{Sp}, I_{COR}^{V} = integrated intensity, corrected for absorption and background of the neutrons scattered quasielastically at the specimen or elastically at the vanadium scatterer.

Refer to the last section of this chapter with regard to the terms elastic and quasielastic.

For the determination of I_{COR}^{Sp} and I_{COR}^{V}, the corresponding spectra of the single detectors in the so-called elastic channels are to be summed. The position of the elastic channels was obtained from the primary spectrum determined from the primary beam with the aid of the transmission monitor, which was also run in a time-of-flight mode.

To separate the quasielastic from the inelastic scattered neutrons, only those pulses were regarded which contribute to that half of the elastic line which lies in the direction of the longer times of flight or larger channel numbers. This part of the elastic line certainly contains no inelastically scattered neutrons since practically no loss scattering occured in the specimens under investigation because of the low primary energy E_0.

See Ref.[5] concerning the energy resolution of the spectrometer at the elastic line. The line width ΔE with the primary energy $E_0 = 1.3$ meV amounted to 0.68 meV. If line broadening occurs by quasielastic scattering which is caused by diffusion within the specimen the relation

$$E = 2\hbar D\kappa^2 \text{ holds.}$$

With $D = 5.10^{-5}\ \frac{cm^2}{sec}$, which is normal for molten metals, we obtain $\Delta E = 0.006$ meV for $\kappa = 0.1$ Å^{-1} and $\Delta E = 0.39$ meV for $\kappa = 0.8$ Å^{-1}. This example shows that the determination of diffusion coefficients by means of this spectrometer is not possible. The calculations are in agreement with the measurements; line broadening of the elastic line could not be observed, furthermore only the resolution function of the spectrometer was observed.

4. RESULTS AND DISCUSSION

Nine different alloys were investigated, the experimental temperature always being 5° C above the liquidus temperature. In addition, the temperature dependency was measured for the alloys containing 50 and 60 at.% Bi.

4.1 Time of flight spectra

Figures 4a and b show time-of-flight spectra for the Bi-Cu melts together with the corresponding concentrations which were obtained from the counter which was mounted at the scattering angle $2\theta = 18{,}7°$. In each case the content of the channel is plotted versus the number of the channel, which is proportional to the time of flight. All spectra show an inelastic (channel number 10 to 30) and a quasielastic region (channel number 30 to 60). The inelastic part is located at smaller times of flight, which means that all inelastically scattered neutrons have gained energy. Practically no loss scattering is observed. The inelastic region of the spectra shows no concentration dependency; there is only a slight shift to lower channels in the case of alloys with higher Cu concentrations. The quasielastic part of the spectra, however, depends very strongly on concentration. The quasielastic peak, which is a measure of local fluctuations within the melt, becomes very strong, especially for the middle concentrations. In contrast, the melts in the copper- or bismuth-rich region of the concentration range show a rather small quasielastic peak.

Figures 5a and b show time-of-flight spectra for different scattering angles 2θ of an alloy containing 50 at. % Bi, which was investigated at a temperature

(a)

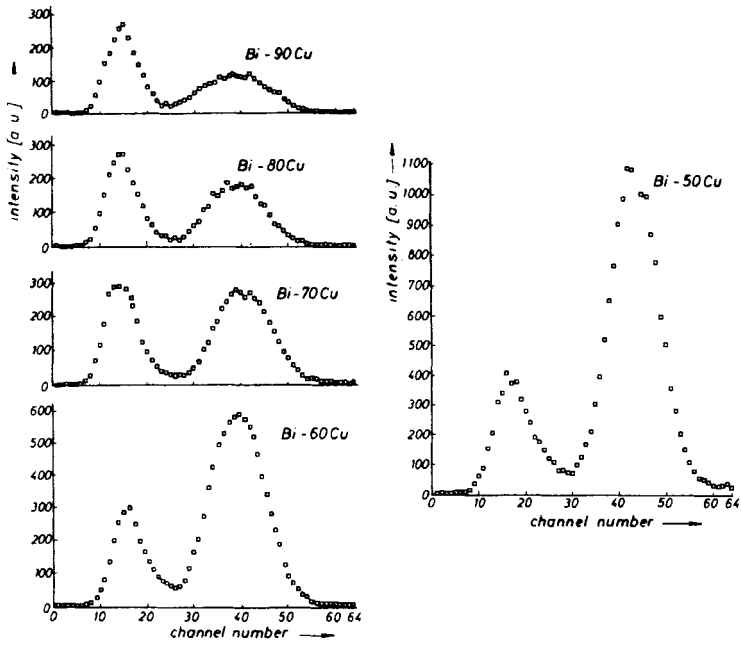

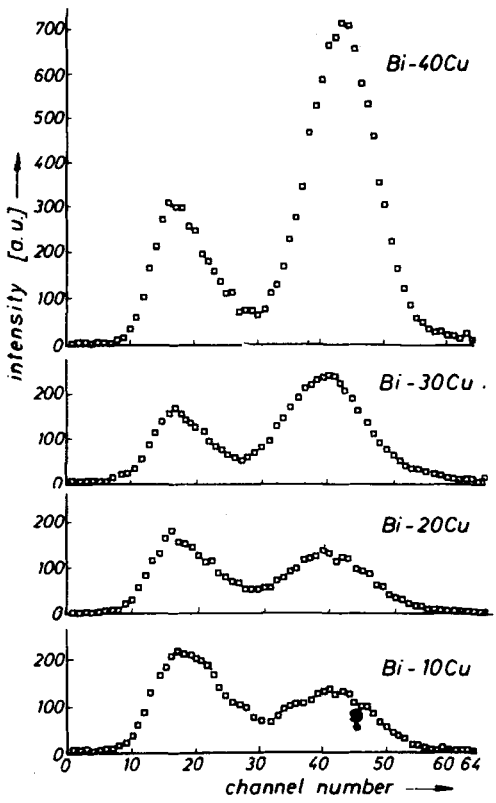

FIGURE 4a + b Time-of-flight spectra of the investigated melts at $2\theta = 18.7°$.

of 830° C, the specimen being vertical to the beam. The value between square brackets is the momentum transfer κ for quasielastic scattering calculated according to the relationship $\kappa = 4\pi \frac{\sin \theta}{\lambda_0}$. The spectra show for small scattering angles 2θ an inelastic and a quasielastic peak With increasing scattering angle, the intensity of the latter decreases. For scattering angles $2\theta > 110°$, it is practically only the inelastically scattered neutrons that are counted. Multiply inelastically scattered neutrons also occur within this region of the spectrum (see Ref.[22]).

Spectra comparable to those presented in Figures 5a and b were also obtained by Wignall and Egelstaff[2] with molten alloys of the systems Bi-Ga, Ga-Pb, and Bi-Zn. Only a few concentrations near the critical point were examined during those investigations.

4.2 Coherent scattering cross sections

Using Eq. (19), the coherent scattering cross sections were calculated for the different melts from the quasielastic scattering. The effect of local temperature fluctuations on the quasielastic scattering is treated with the aid of Eq. (20), where the corresponding cross section in the direction of the primary beam is defined as:

$$\left.\frac{d\sigma(0)}{d\Omega}\right|_{COH}^{temp.} = \rho_0 k_B T \chi_T \left(1 - \frac{c_v}{cp}\right) \cdot \langle b \rangle^2 \tag{20}$$

The thermodynamic data necessary for its determination were taken from Ref.[32]. For all alloys under investigation, the values obtained for this scattering cross section are below $5 \frac{\text{mbarn}}{\text{sterad.atom}}$. These figures are negligibly small compared with the values determined experimentally. This scattering cross section from temperature fluctuations becomes remarkable at the liquid-gas phase transition, where the isothermal compressibility and also cp become very large.

Thus, we can conclude that the coherent scattering cross sections determined during the present work and presented in Figures 6a and b are caused by the concentration fluctuations. All alloys show an increase of the scattering cross section with decreasing κ, but this increase is small for the Cu-rich and the Bi-rich alloys, while considerable for the alloys in the middle concentration range. The further evaluation of these curves will be presented in sections 4.3 and 4.4.

(a)

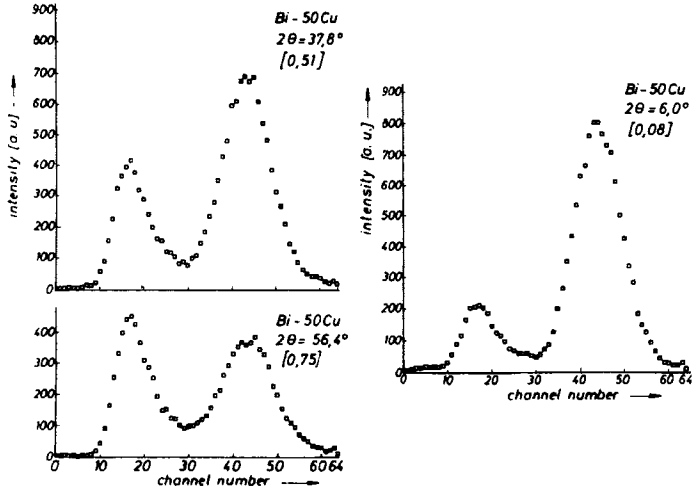

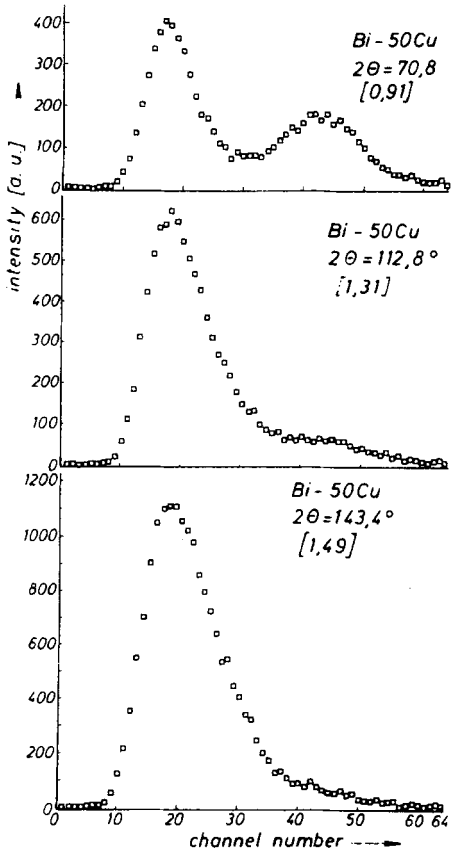

FIGURE 5a + b Time-of-flight spectra of a Bi-Cu melt with 50 at.% Bi for different scattering angles.

Further measurements at higher temperatures were done to determine the temperature dependency of $\left.\frac{d\sigma(0)}{d\Omega}\right|_{COH}$ in the alloys containing 40 and 50 at.% Cu. Both alloys show the same temperature dependency, namely a decrease of the scattering cross section in the direction of the primary beam with increasing temperature.

Figure 7 shows the temperature dependency of the macroscopic scattering cross section $\frac{d\Sigma}{d\Omega} = \rho_0 \left.\frac{d\sigma(0)}{d\Omega}\right|_{COH}$ of both alloys. There is a linear relation in the temperature range between 800° C and 1100° C. The upper limit is given by the experimental device. The alloy with 50 at.% Cu shows a larger

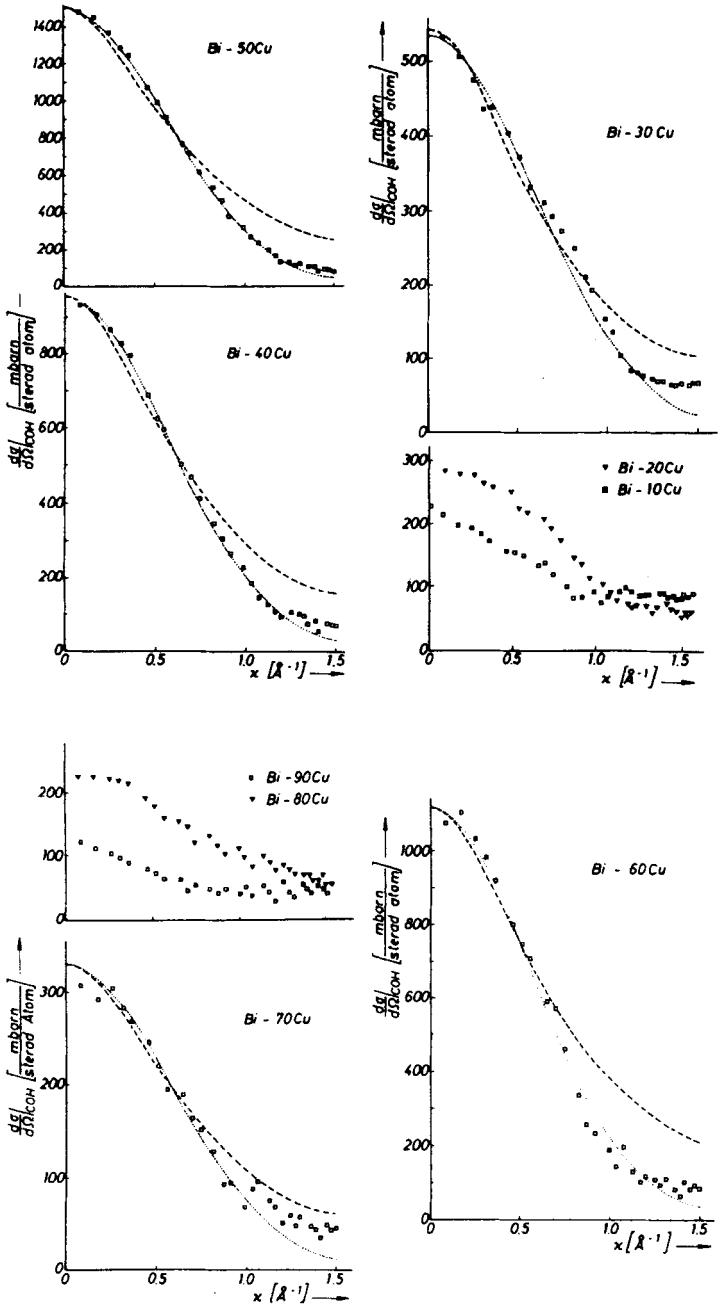

FIGURES 6a + b Coherent scattering cross section
□ experimental
· · · calculated according to Guinier
--- calculated according to Ornstein-Zernike.

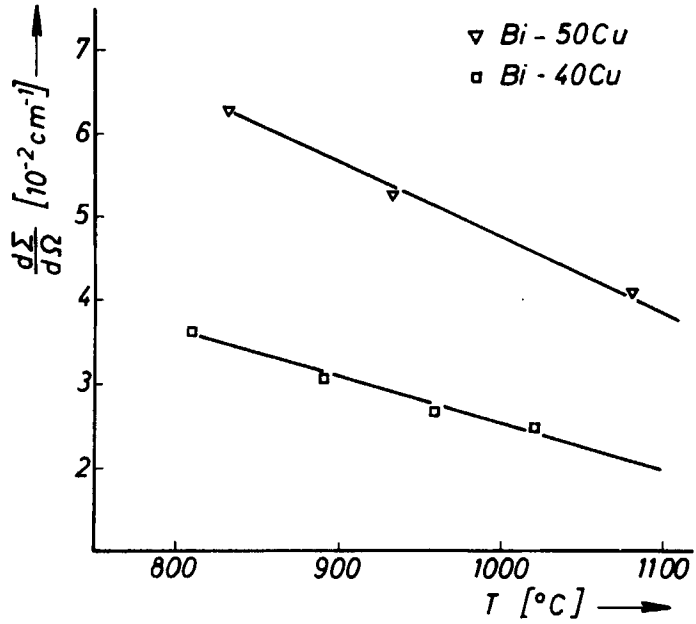

FIGURE 7 Temperature dependency of the scattering cross section in direction of the primary beam.

decrease of $\frac{d\Sigma}{d\Omega}$ with increasing temperature than the alloy with 40 at.%. The linear extrapolation of both straight lines in Figure 7 shows that they reach the value $\frac{d\Sigma}{d\Omega} = 10^{-2}\ cm^{-1}$, which is valid for the Cu- or Bi-rich alloys, at temperatures of approximately 1300 to 1400° C. Thus, we come to the result that the concentration fluctuations have vanished at about 1350° C, i.e. 200° C below the boiling point of Bi.

4.3 Ornstein-Zernike method

As described in Section 2.2a, the mean dimensions of the concentration fluctuations are obtained by plotting $\left(\frac{d\sigma(\kappa)}{d\Omega}\Big|_{COH}\right)^{-1}$ versus κ^2. This was done for the alloys with concentrations between 30 and 70 at.% Bi. The correlation lengths ξ obtained from these so-called Ornstein-Zernike plots are plotted in Figure 8 versus the Bi concentration. Apparently, the correlation length is nearly independent of alloy composition.

The coherent scattering cross section for concentration fluctuations was now calculated using Eq. (13), where the correlation length ξ and the

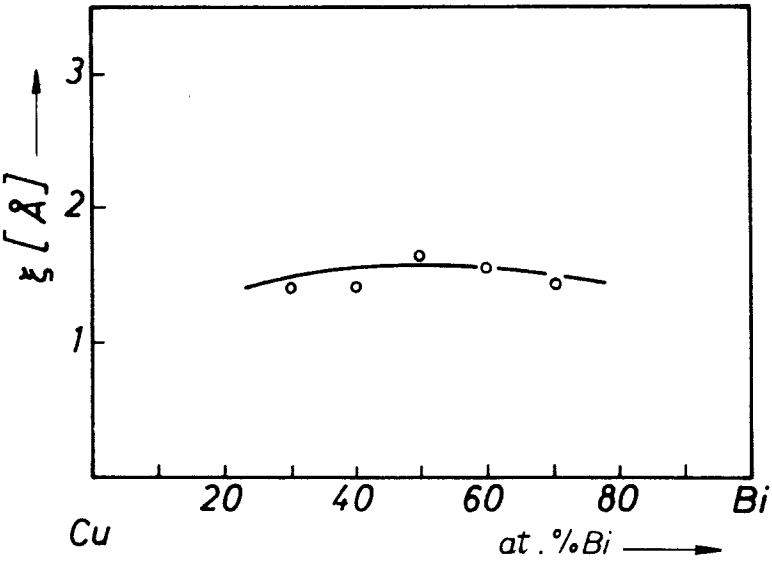

FIGURE 8 Correlation length.

scattering cross section in the direction of the primary beam were taken from the corresponding figures. The results are plotted in Figures 6a and b with dashed lines. Apparently, the scattering cross section can be described up to $\kappa \approx 0.7$ Å^{-1} using the Ornstein-Zernike method. A similar behaviour was found by Egelstaff and Wignall[24] with a molten Bi-83 Zn alloy. A deviation between the experimental curve and that calculated using the Ornstein-Zernike method could also be observed in that case above $\kappa = 0.9$ Å^{-1}. The reason lies in the fact that the Lorentz function, which is used by Ornstein-Zernike to represent the scattering caused by concentration fluctuations, can only describe the asymptotic behaviour of the cross section for $\kappa \to 0$ (see Ref.[25]).

4.4 Guinier method

A further possibility to obtain a quantitative measure of the dimensions of inhomogeneities from the scattering curves is given by the so-called Guinier approximation, which was described in Section 2.2b. Besides the dimensions of the particles, their shape can also be determined by this method. The radius of gyration R_g can be determined from the gradient of the straight line which is obtained by plotting the logarithm of the scattering cross section versus κ^2. Small deviations from the straight line could be observed for $\kappa > 1$ Å^{-1} in the present case. In this range the statistical error is rather high, because the spectrum shows only small intensities.

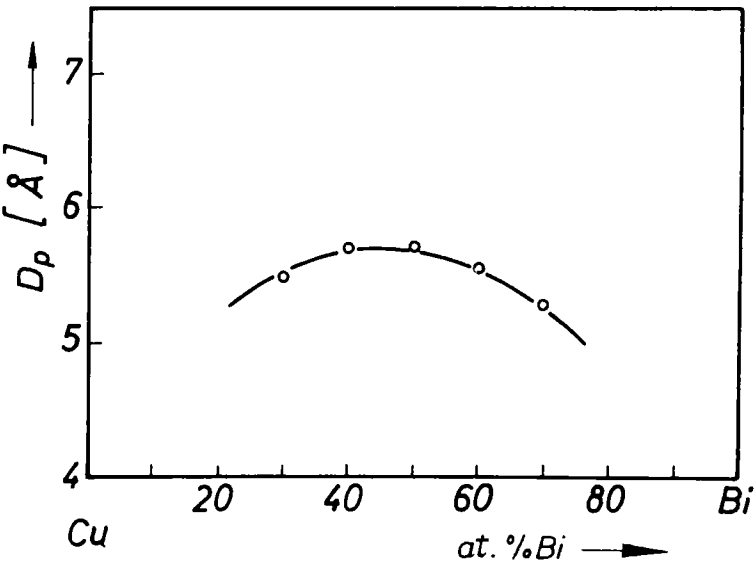

FIGURE 9 Particle diameter.

Since no direction is preferred within a melt the inhomogeneities can be taken as small spheres, whose radii can be calculated from the radius of gyration using Eq. (16). Figure 9 shows the diameter of particles versus the Bi concentration. The radius shows a slight concentration dependency and has its largest value of 5.8 Å for the middle concentrations. Thus, the submicroscopic segregation within the molten Bi-Cu alloys is limited to the first coordination shell[1]. For the Al-Sn or Al-In systems, particle diameters of about 10 Å were obtained[3 or 4].

According to Eqs. (14) to (16), the scattering cross section in Guinier's approximation can also be presented in the form

$$\left.\frac{d\sigma(\kappa)}{d\Omega}\right|_{COH}^{P} = \frac{1}{\rho_0}\frac{d\Sigma}{d\Omega}\exp\left[-\frac{R_p^2}{5}\kappa^2\right] \tag{21}$$

This cross section was calculated for the alloys between 30 and 70 at.% Bi with the corresponding values for $\frac{d\Sigma}{d\Omega}$ and R_p and is also plotted in Figs. 6a and 6b. Thus, for the region $\kappa < 1$ Å^{-1} a good agreement between the experimental values and the values according to Guinier's approximation is obtained for all alloys. Nevertheless, the application of this method of evaluation to melts has to be critically thought over.

Concerning the temperature dependency of the particle diameters, it should be pointed out that these remain rather constant. The evaluation of

the scattering curve of the alloy with 50 at.% Bi yielded at 1080° C a particle diameter of 5.4 Å, at 830° C one of 5.8 Å. This means a decrease of less than 10% of the particle diameter during an increase in temperature of about 250° C. The same holds for the temperature dependency of the correlation lengths (refer to Eq. (22)).

The evaluation using Ornstein-Zernike and Guinier methods has shown that the experimental scattering cross sections can be well approximated by both methods in certain κ-regions. To get at least qualitative agreement between D_p and ξ, the scattering functions of both methods are transformed to correlation functions. Defining the mean dimension of a segregated zone in such a way that the correlation function has decreased to e^{-1} at the boundary of this zone, we obtain

$$D_p = \sqrt{5} \cdot \xi \tag{22}$$

As can be seen from Figs. 8 and 9 this condition is not fulfilled exactly for Bi-Cu melts, but qualitative agreement is found. Refer to the following work Ref.[26] for the further evaluation of the scattering cross section $\frac{d\Sigma}{d\Omega}$ in the direction of the primary beam.

Acknowledgements

We wish to thank Prof. Dr. W. Schmatz, Institut für Festkörperforschung, Jülich, for his numerous suggestions and discussions, and the Deutsche Forschungsgemeinschaft for financial support.

References

1. W. Zaiss and S. Steeb, Phys. Chem. Lig. *5*, (1976).
2. G. D. Wignall and P. A. Egelstaff, *J. Phys. C.* **1**, 1088 (1968).
3. R. Hezel and S. Steeb, *Z. Nat. forschung* **25a**, 1085 (1970).
4. J. Höhler and S. Steeb, *Z. Nat. forschung* **30a**, 775 (1975).
5. G. S. Bauer, Dissertation Univ. Bochum (1975). Report KFA Jûlich, Jül. 1158, 1975.
6. A. Guinier and G. Fournet, "Small Angle Scattering of X-Rays", Wiley, New York (1955).
7. W. Schmatz, T. Springer, J. Schelten, and K. Ibel, *J. Appl. Cryst.* 7, 96 (1974).
8. H. Ruppersberg, *Phys. Letters* **46A**, 75 (1973).
9. A. B. Bhatia and D. E. Thornton, *Phys. Rev. B*, **2**, 3004 (1970).
10. L. Landau and E. Lifschitz, "Statistical Physics", Addison-Wesley Publishing Co., Mass. (1958).
11. T. Springer, in "Springer Tracts in Modern Physics", **64**, Springer-Verlag, Berlin (1972).
12. P. A. Egelstaff and J. W. Ring, in "Physics of Simple Liquids" ed. H. N. V. Temperley, J. S. Rowlinson and G. S. Rushbrooke, North Holland, Amsterdam (1968), S.253.
13. L. S. Ornstein and F. Zernike, *Phys. Z.* **19**, 134 (1918).
14. M. E. Fisher, *J. Math. Physics* **5**, 944 (1964).
15. S. Komura, G. Lippmann, and W. Schmatz, *J. Appl. Cryst*, **7**, 233 (1974).
16. J. H. Raynal, J. Schelten, and W. Schmatz, *J. Appl. Cryst.* **4**, 511 (1971).
17. S. J. Cocking, in "Properties of Liquid Metals", S.198, ed. P. D. Adams, H. A. Davis, and S. G. Epstein, Taylor u. Francis, London (1967).

18. N. Mateescu, in "Inelastic Neutron Scattering in Solids and Liquids", S.431, IAEA, Wien (1968).
19. W. Zaiss, Dissertation, Universität Stuttgart (1975).
20. H. G. Mayer, A. Koeppe, and R. Schäfer, *high temp. high press.* **6**, 383 (1974).
21. K. Sagel, Tabellen zur Röntgenstrukturanalyse, Springer-Verlag, Berlin (1958).
22. S. J. Cocking and P. A. Egelstaff, *J. Phys. C.* **1**, 507 (1968).
23. H. Ebert, J. Höhler, and S. Steeb, *Z. Nat. forschung* **29a**, 1890 (1974).
24. P. A. Egelstaff and G. D. Wignall, A.E.R.E. Rep. No. 5627 (1967).
25. A. Münster and C. Schneeweiss, *Z. Phys. Chem.* **37**, 353 (1963).
26. W. Zaiss and S. Steeb, Phys. Chem. Liq. *5*, 111 (1976).